Differential Gain Enhancement in a Quantum Dash Laser Using Strong Optical Injection

L. F. Lester[1], F. Grillot[2] , N. A. Naderi[1], and V. Kovanis[3]
[1]Center for High Technology Materials, University of New Mexico, 1313 Goddard SE, Albuquerque, NM 87106, USA.
[2]Telecom Paristech, Ecole National Supérieure des Télécommunications, CNRS LTCI, 75634 Paris Cedex, France
[3]Air Force Research Laboratory, 2241 Avionics Circle, Wright -Patterson AFB, Dayton, OH 45433, USA
Tel : (505)-272-7800 Fax: (505)-272-7801, email: lflester@unm.edu

ABSTRACT

Increased differential gain is typically realized through strain, quantum confinement, or p-type doping in the active region. These methods have been applied to quantum dots or dashes to raise the differential gain with limited success because the optical gain of these low dimensional systems saturates at modest values. Instead larger differential gain can be accessed at wavelengths blue-shifted from the gain peak and close to optical transparency using the threshold shift induced by optical injection. Using these approaches, greater than 50X improvement in the differential gain has been achieved in an injection-locked QDash FP laser compared to its free-running value.

Keywords: Semiconductor lasers, quantum dots, optical injection, differential gain, linewidth enhancement factor.

1. INTRODUCTION

The 3-dB modulation bandwidth and linewidth enhancement factor (LEF) of a semiconductor laser both directly benefit from an increased differential optical gain, which is typically improved through the use of strain[1], quantum confinement[2], or p-type doping[3] in the active region of the device. All of these methods have been applied to quantum dot or dash materials to raise the differential gain, but unfortunately these low-dimensional systems have relatively small optical gain. The result is that the laser cavity has to be relatively low-loss, which might make the LEF smaller, but comes at the expense of the modulation bandwidth since the photon lifetime is longer. The challenge is to access the large differential gain available in a quantum dot at a low optical gain value without sacrificing the photon lifetime. Strong optical injection is a possible method to accomplish this goal because it is capable of shifting the laser threshold close to optical transparency. Also, larger differential gains are found at wavelengths blue-shifted from the gain peak. Using this approach and strong injection, more than 50X improvement in the differential gain is shown in an injection-locked QDash Fabry-Perot laser compared to its free-running value. Furthermore, the injection-locked system's 3-dB bandwidth enhancement, flat modulation response profile, and extremely low LEF are investigated using a set of analytical equations derived for the zero-detuning, zero-LEF case. From an applications perspective, the combination of an enhanced bandwidth and a very low α-factor is promising for improving transmitter modules for future long-haul and high-speed optical fiber links.

Quantum nanostructure-based lasers have been predicted to have superior dynamic properties compared to Quantum-Well (QW) or bulk lasers making them attractive candidates for many applications such as high-speed sources in optical communication systems[4, 5, 6]. And tunable photonic oscillators for low phase noise clocks for precession time applications [xxx, xxx]. All of these properties have been experimentally verified on actual quantum-dot (QD) or quantum-dash (QDash) laser devices; including ultra-low transparency current density[7], and low temperature dependence of threshold current density[8]. In addition to the advantages mentioned above, nanostructure lasers have also been touted to exhibit an increased gain and differential gain[9] as well as a reduced linewidth enhancement factor[10] (α-*factor*), which in theory make them even more suitable for implementation in ultrafast and chirp-free transmitter modules. In reality, it is well known that the latter properties are not necessarily

Physics and Simulation of Optoelectronic Devices XX, edited by Bernd Witzigmann, MarekOsinski, Fritz Henneberger, Yasuhiko Arakawa, Proc. of SPIE Vol. 8619, 8619-6

accessible at the same time in nanostructure gain media. In another word, achieving a simultaneous high 3-dB modulation bandwidth (f_{3dB}) and chirp-free operation in conventional directly modulated lasers, if theoretically proven to be possible, practically is very challenging.

The modulation bandwidth of nanostructure lasers on one hand is inherently limited by several factors such as phonon bottleneck associated with relatively slow carrier relaxation time[11], the inhomogeneous gain broadening[12] and hot carrier effects[13]. For instance, the inhomogeneous broadening associated with nanostructure size dispersion is ultimately limited by growth technology and it causes both the optical gain and differential gain to reduce in the active region. In addition, strong gain saturation in QD gain media at higher current injections can significantly hinder the maximum achievable f_{3dB} in such devices. As a result, f_{3dB} of conventional separate confinement heterostructure (SCH) QD lasers is limited to only 5-8 GHz[14, 15].

On the other hand, the ultra-low *α-factor* benefit intrinsic to nanostructure gain media is no longer available at high current densities where the large bandwidths are accessible. Although below-threshold measurements on QDs[16, 17] have reported *α-factors*, both negative and less than 1, on the contrary, the above-threshold values are found to be much larger as a result of carrier density being unclamped at threshold which is due to the inhomogeneous gain broadening in dots. In addition, at higher current densities, *α-factor* becomes more power dependent due to strong gain saturation and carrier filling in both lasing and non-lasing QD states[18, 19].

In this work, we experimentally demonstrate and theoretically analyze that both f_{3dB} and the above-threshold *α-factor* can be simultaneously improved by accessing large differential gain values available in the nanostructure gain media. To date, several methods, including p-type doping of gain region, have been applied to both QD or QDash materials to access larger differential gain values[20, 21], but unfortunately increased gain compression and thermal broadening effects due to high absorption counteract this benefit. In addition, these low-dimensional systems have relatively small optical gain. The result is that the laser cavity has to be relatively low-loss, which might make the the differential gain larger and the *α-factor* smaller, but comes at the expense of the bandwidth since the photon lifetime is longer. The challenge here is to access the large differential gain available in a quantum dot gain medium at a low optical gain value without sacrificing the photon lifetime. Strong optical injection is a possible method to accomplish this goal because it is capable of shifting the laser threshold close to optical transparency[22, 23]. Also as predicted by theory, larger differential gains are found at wavelengths blue-shifted from the gain peak[24]. This paper examines the effect of these approaches on a quantum dot gain medium, specifically a quantum dash one which is essentially an elongated dot structure.

2. RESULTS and DISCUSSION

Here, we study the manipulation of the slave laser's differential gain and the resulting *α-factor* in a QDash Fabry-Perot (FP) laser with optical injection using two different approaches. First, using the amplified spontaneous emission (ASE) technique[25], the QDash net modal gain profile is separately measured as a function of wavelength and current density. Knowing such a dependence is critical in identifying the optimum free-running operating point at which the *α-factor* can be manipulated to its lowest possible values under optical injection. Then, using the ratio of the frequency modulation (FM) to the amplitude modulation (AM) indices technique[26], the above threshold *α-factor* is directly measured under injection-locking at zero-detuning as the injected power is varied. Second, measured experimental modulation response data is used to extract the relevant operating parameters of the coupled system including the threshold gain shift and *α-factor*, as it is further described in Supplementory Information. The FM/AM measured α-factor values are then compared with the extracted values and the results are correlated with the threshold gain shift caused by optical injection at zero-detuning. Emphasis on the zero-detuning case is mainly based on two reasons. First, the zero-detuning case simplifies the theoretical model describing the behavior of the coupled system under modulation, making it easier to simulate and extract the operating parameters of the locked system from measured response data. Second, this case demonstrates a relatively flat modulation response compared to other detuning conditions making it most suitable for broadband applications. From an implementation perspective, the master and slave lasers can be referenced to the same wavelength locker, facilitating implementation in a compact butterfly package suitable for high-speed applications in optical fiber links.

Figure 1 illustrates the epitaxial layer structure and atomic force microscope (AFM) image of the InAs QDash laser device under the investigation. The laser material was grown by molecular-beam epitaxy (MBE) on an n^+-InP

(001) substrate. The active region (shown in Fig. 1) is a dash-in-a-well (DWELL) consisting of five stacks of InAs quantum dashes embedded in compressively-strained $Al_{0.20}Ga_{0.16}In_{0.64}As$ quantum wells. Each quantum well is separated by 30-nm wide undoped, tensile-strained $Al_{0.28}Ga_{0.22}In_{0.50}As$ spacers on both sides of the DWELL active region. Lattice-matched $Al_{0.30}Ga_{0.18}In_{0.52}As$ waveguide layers of 105 nm are added on each side of the active region. The 1.5-μm thick AlInAs p-cladding layer is beryllium (Be) step-doped to reduce the free-carrier losses. The n-cladding layer is 500-nm thick AlInAs. The laser structure is capped with a 100-nm thick p^{++}-InGaAs layer. Four-micron wide ridge waveguide FP laser bars were fabricated using standard processing techniques and cleaved into 500-μm long cavity lengths. The nominal emission wavelength of the laser is around 1567 nm, the threshold current was measured to be 54 mA ($J_{th} \sim 2700$ A/cm^2) with a slope efficiency of 0.2 W/A at room temperature. The data for the net modal gain as a function of wavelength for various injected current densities are shown in Figure 2, indicating the QDash nominal gain peak at 1565nm at room temperature. When the slave laser is injection-locked, since the injected light by the master laser is at a fixed wavelength and increasing injection strength shifts the slave's threshold condition to lower pump values, the *α-factor* is expected to progressively decrease with injection as operation is more and more on the blue side of the gain peak. In addition, the *α-factors* at all wavelengths generally decrease with a lower threshold condition in dashes because of lower carrier population in the excited states[17]. The QDash *α-factor* is then measured under injection-locking at 1550nm and 1535nm for zero-detuning cases as the injected power is varied. The injection-locking experimental setup for measuring the *α-factor* using the FM/AM technique is shown in Figure 3.

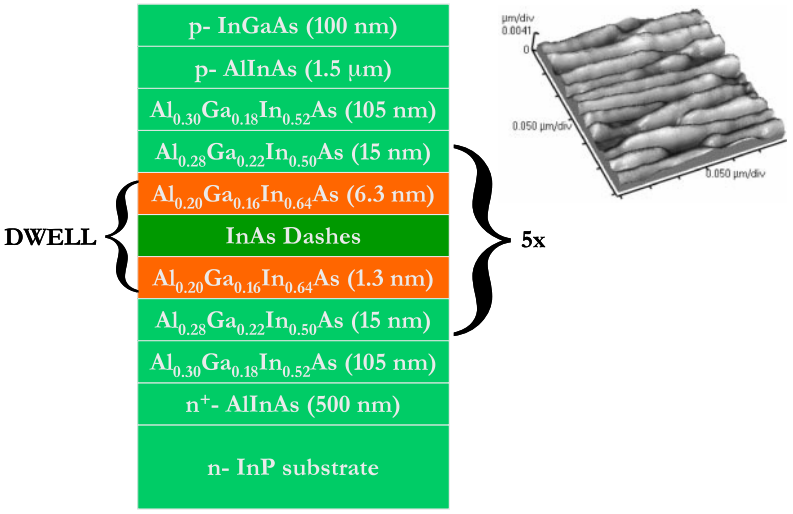

Figure 1: The epitaxial structure of the InAs quantum dash laser structure with a typical AFM trace on the right.

The injection-locking experimental setup for measuring *α-factor* using the FM/AM technique and the modulation response is shown in Fig. 3. The experimental setup relies on the use of a tunable master laser, an optical circulator, a polarization controller, a band-pass filter and an erbium-doped fiber amplifier (EDFA). For this study, the slave laser was DC biased slightly above threshold at 60 mA and directly modulated. The modulated signal was provided via the internal RF source in the network analyzer where it was also mixed with the DC current through the integrated bias-tee. An 18 GHz RF signal amplifier was provided at RF port 1 of the modulation setup to adjust the RF power as needed. To prevent the second harmonic generation by the RF source a 20 GHz low-pass filter was used after the amplifier. The output power of the slave laser is carefully coupled into a single-mode polarization maintaining (PM) lensed fiber using the piezoelectric stage controller. The anti-reflection (AR) coated PM lensed fiber is connected to port 1 of a 3-port PM circulator. The optical circulator serves as the core of the injection-locked setup such that it provides the desired propagation path for the optical signal and blocks undesired light from coupling into the slave and master lasers. Depending on the operating wavelength of the slave laser under test, the tunable master laser's wavelength was adjusted appropriately. The master laser used for this experiment was a tunable external cavity laser with a single-mode PM fiber pigtail connected to port 2 of the circulator. The tunable laser operates at wavelength range from 1530 nm to 1580 nm with a 10 pm tuning resolution. The injection-locking

setup used in this study is capable of maximum amplified optical power of 9.3 dB, which was limited by overall 5 dB loss resulting from the polarization controller, band-pass filter and fiber connectors. In all of the injection-locking cases, the external power ratio, R_{ext} (master to slave optical power ratio at external slave facet), was varied between -3.8 dB to 9.3 dB using a C or L-band optical amplifier. At port 2, the master laser was connected to the amplifier capable of outputting a maximum power of 100 mW to boost the optical signal from the master laser at a desired wavelength. The amplifier noise is reduced by using a band-pass filter. After the band-pass filter, a free-space polarization controller is used to ensure that the injection field polarization was controlled from the master laser. Port 3 of the circulator was connected to the high-speed detector through which the relative modulation response ($|S_{21}|^2$) was measured using the network analyzer. The 50/50 beam splitter at port 3 of the circulator is used to measure the modulation response of the injection-locked laser while simultaneously monitoring the frequency detuning between the master and slave lasers. The high-resolution spectrometer (HRS) is used to determine the frequency offset between the master and slave lasers (i.e. zero-detuning), as well as to identify stably-locked conditions.

The FM/AM modulation method relies on the high-frequency small-signal modulation of the carrier density of the laser obtained by modulation of the bias current. Since the gain and refractive index are both carrier density dependent, modulation of carrier density will generate amplitude and frequency modulation in the output signal. From the small-signal modulation analysis, the ratio of the FM/AM modulation indices provides a direct measurement of the above threshold *α-factor* for modulation frequencies well above the slave laser's relaxation frequency[26]. Using this method, the AM index, was modified through the ratio of the ac and dc components of the detected modulated signal using an electrical spectrum analyzer (ESA) and a 50 Ω terminator connected to a high-speed photo-detector. While the external power ratio was varied, the AM index was kept constant at 6% for all injection-locking case by adjusting the RF power output from the amplifier. The FM index, was obtained by measuring the ratio between amplitudes of the nearest sidebands to the peak frequency using a high-resolution spectrometer.

For comparison and to confirm the accuracy of the measured *α-factor* values, the experimental modulation response data at each zero-detuning case is used to extract the relevant operating parameters of the system including the *α-factor* and the corresponding threshold gain shift.

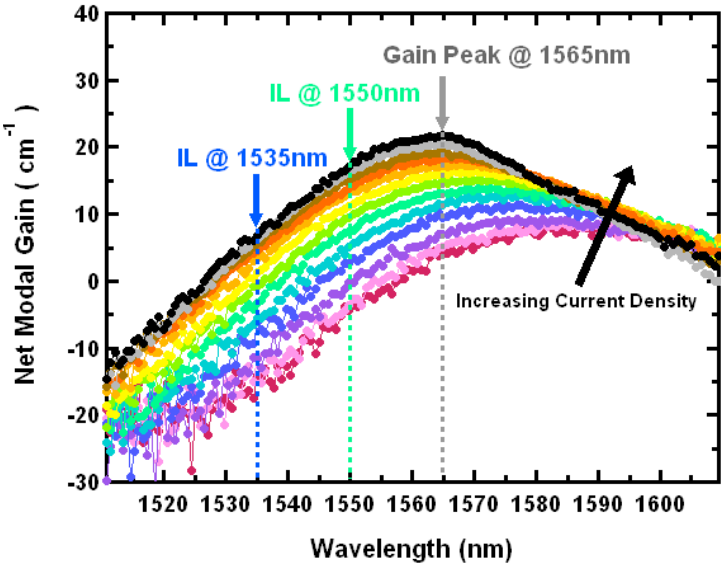

Figure 2: The measured net modal gain curves as a function of wavelength and current density. Several wavelengths are identified with arrows at which injection locking at the nearest Fabry-Perot mode was undertaken.

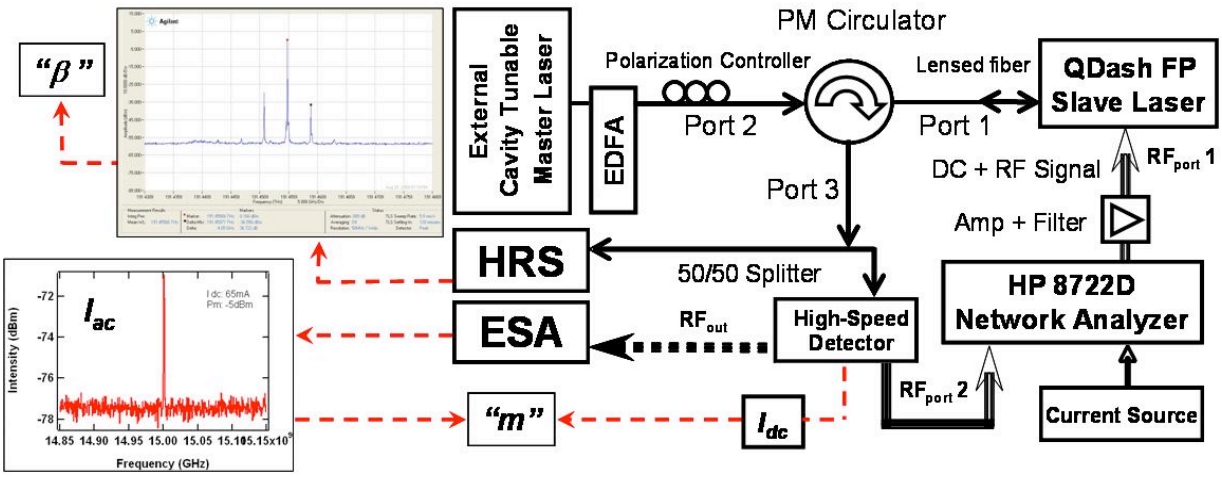

Figure 3: The optical injection setup showing the various pieces of diagnostic equipment. HRS stands for high resolution spectrometer. ESA is an electrical spectrum analyzer.

The modulation response of an injection-locked coupled system is described by the following equations[27]:

$$|H_R|^2 = 10\log\left[\frac{\left(\frac{C}{Z}\right)^2\left(\omega^2+Z^2\right)}{\left(C-A\omega^2\right)^2+\left(B\omega-\omega^3\right)^2}\frac{1}{\left(1+\left(\omega/\gamma_c\right)^2\right)}\right]$$

$$A = (\gamma_{fr}-\gamma_N)R_{FE}^2+\gamma_N+\gamma_{th}$$

$$B = \left(\omega_r^2+\gamma_N\gamma_{th}\right)+\left(\eta_0/R_{FE}\right)^2+\gamma_{th}\left[\left(\gamma_{fr}-\gamma_N\right)R_{FE}^2+\gamma_N\right]$$

$$C = \left(\eta_0/R_{FE}\right)^2\left[(\gamma_{fr}-\gamma_N)R_{FE}^2+\gamma_N\right]-\left(\omega_r^2+\gamma_N\gamma_{th}\right)Z$$

where ω_r, γ_{fr}, γ_N, and γ_c are the free-running relaxation frequency, free-running damping rate, inverse differential carrier lifetime and inverse RC parasitic roll-off, respectively, and are known parameters of the slave laser. The non-linear gain has been implicitly incorporated into the model through the free-running relaxation oscillation and damping rate[27]. Parameter η_0 denotes the maximum injection strength controlled by the experiment and calculated using the coupling efficiency, η_c, the external power ratio, R_{ext}, cavity length, L, and front facet reflectance, r, of the FP slave laser. The external power ratio, R_{FE} is the slave field enhancement factor that takes into account the deviation of the steady-state field magnitude compared to its free-running value at high injection ratios[27]. The frequency detuning is defined as $\Delta\omega = \omega_{slave} - \omega_{master}$. The steady-state phase offset between the master and slave under the zero-detuning case is given by $\phi_0 = -\tan^{-1}(\alpha)$, reducing Z and γ_{th}, the threshold gain shift to:

$$Z = \frac{-\eta_o}{R_{FE}}\sqrt{1+\alpha^2} \qquad \gamma_{th} = \frac{2\eta_o}{R_{FE}\sqrt{1+\alpha^2}}$$

When using these equations to curve-fit measured response data, the number of fitting parameters is reduced using the known free-running terms and by applying proper constraints on η_0, R_{FE} and γ_{th}. The *α-factor* parameter is directly extracted using a fitting-algorithm[27]. The initial guess value for the field enhancement factor R_{FE} can be calculated in the fitting function by solving a quadratic expression arising from the steady-state slave field expression and the simplified expression for γ_{th} at zero-detuning; R_{FE}^4-[$(1/\gamma_p)(2\eta_0/(1+\alpha^2)^{1/2})$+1] R_{FE}^2- $(\gamma_N/\omega_r^2)(2\eta_0/(1+\alpha^2)^{1/2})$. Using the measured FM/AM values, the *α-factor* is allowed to fluctuate between a reasonable positive and negative range during the least-squares-fitting process. Both the *α-factor* and γ_{th} are directly extracted using the modulation response function presented above.

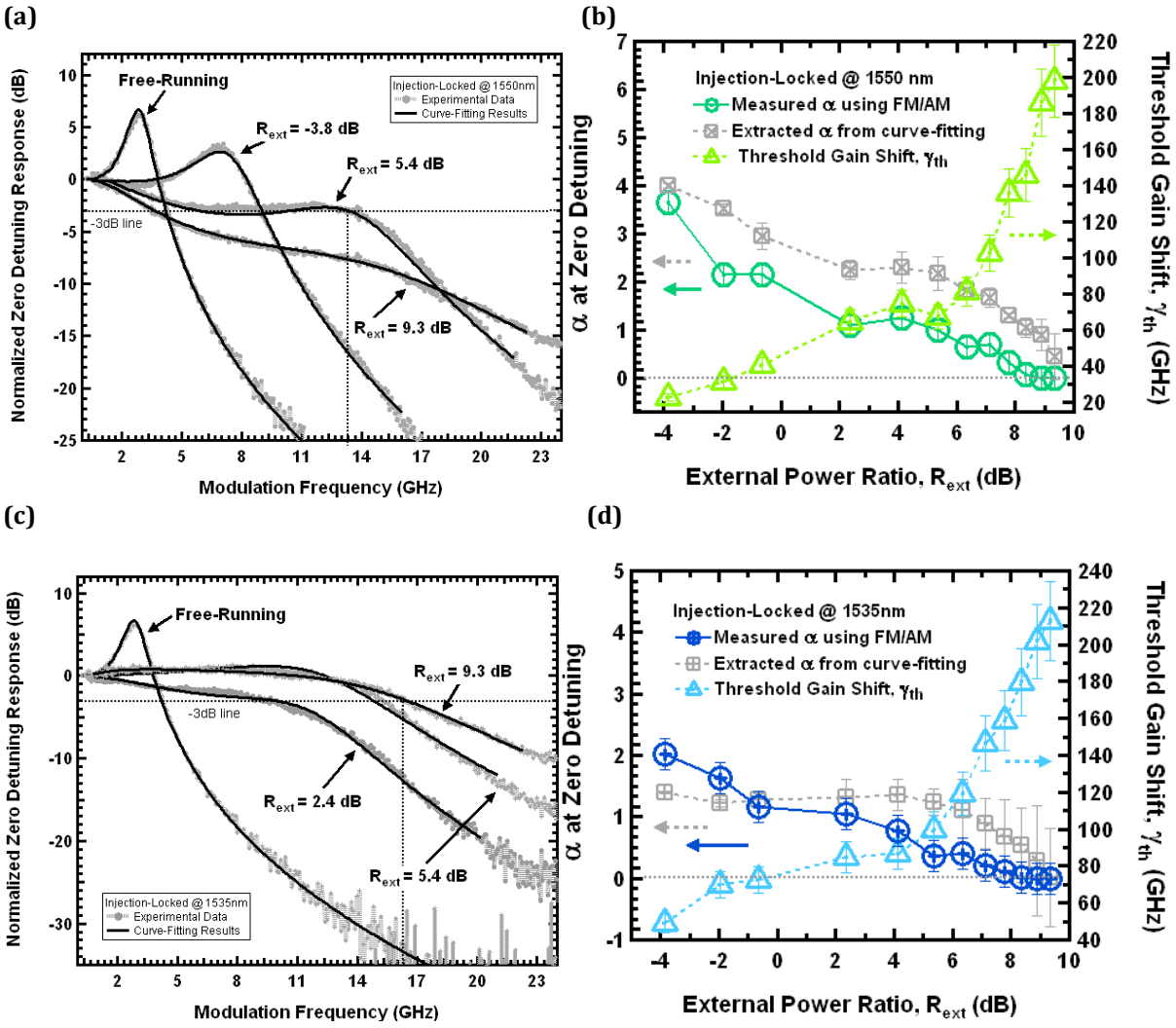

Figure 4: Modulation characteristics and operating parameters of injection-locked QDash laser as a function of external injection ratio, R_{ext}. **a**, **c**; RF modulation responses of injection-locked QDash FP laser, and **b**, **d**; variation of zero-detuning *α-factor* and threshold gain shift and as a function of external injection ratio respectively at 1550nm and 1535nm FP locked modes. The error analysis for extracted values of *α-factor* and threshold gain shift shown in Figures **b**, and **d**, are calculated based on a one standard deviation confidence interval.

Figures 4a, and 4c show the zero-detuning response data near the gain peak at 1550nm and at a further blue-shifted wavelength of 1535nm for various values of the external master-to-slave power ratio, R_{ext}, ranging from -3.8dB to 9.3dB at the slave arm. A maximum f_{3dB} of 13.3GHz, and 16.3GHz were measured for 1550nm, and 1535nm respectively. Note that the near-flat response for 1535nm at R_{ext}=9.3dB locking case Figures 4a, and 4c show the zero-detuning response data near the gain peak at 1550nm and at further blue-shifted wavelength of 1535nm for various values of the external master-to-slave power ratio, R_{ext}, ranging from -3.8dB to 9.3dB at the slave arm. A maximum f_{3dB} of 13.3GHz, and 16.3GHz were measured for 1550nm, and 1535nm respectively. Note that the near-flat response for 1535nm at R_{ext}=9.3dB corresponds to a 4x improvement compared to the free-running case. To the best of our knowledge this response data is the first of its kind that has ever been observed in such devices. The measured values of the *α-factor* as a function of R_{ext} using the FM/AM technique are shown in Figures 4b and 4d. For comparison, the curve-fits of the responses shown in Figures 4a and 4c, also give the values for *α-factor* and the corresponding threshold gain shifts at both injection-locked cases. The extracted *α-factor* values for both cases are in an excellent agreement with the FM/AM measured values. Also these results indicate significant threshold gain shifts with increased R_{ext} for both locking cases, which explains, in part, the lower *α-factor* values at lower wavelengths

from the gain peak. From the curve-fitting results an *α-factor* of 0.01 (or 0.0 within the curve-fitting error range) was extracted for the zero-detuning case at 1535 nm and R_{ext}=9.3dB. The largest threshold gain shift for the zero-detuning case at 1535nm is 24.6cm^{-1}, which is about 68% of the maximum possible value. The highest threshold gain shift obtained for this case is equivalent to a reduced threshold current density of 1458A/cm^2 and the achievement of a differential gain of 6 x 10^{-14} cm^{-2} represents a greater than 50X increase in differential gain from its free-running value.

3. CONCLUSIONS

We have demonstrated that the use of strong optical injection in nanostructure lasers allows for manipulation of the *α-factor* to near-zero values through the enhancement of the differential gain from its free-running value. This novel finding verifies greater than 50x improvement in the differential gain in an injection-locked QDash FP laser compared to its free-running value as a result of strong optical injection at wavelengths blue-shifted from gain peak and operation near optical transparency. The unique broadband responses, along with their associated ultra-low *α-factors* observed in this work indicate that the optically-coupled nanostructure laser system has the potential to be optimized as an integrated high-speed photonic transmitter to be used in future long-haul and high performance optical fiber links.

ACKNOWLEDGEMENTS

This work was supported by United States Air Force Research Laboratory under grant numbers FA8750-06-1-0085 and FA9550-10-1-0276. V. Kovanis work was supported via the Air Force Office of Scientific Research (AFOSR) Laboratory Research Initiation Request LRIR 09RY04COR.

REFERENCES

[1] Lau, K. Y. *et al.* "Enhancement of modulation bandwidth in InGaAs strained-layer single quantum well lasers," *Appl. Phys. Lett.* **55,** 1173-1175 (1989).

[2] Arakawa, Y., & Yariv, A., "Theory of gain, modulation response, and spectral linewidth in AlGaAs quantum well lasers," *IEEE J. Quantum Electron.* **21,** 1666-1674 (1985).

[3] Vahala, K. J. & Zah, C. E. "Effect of doping on the optical gain and the spontaneous noise enhancement factor in quantum well amplifiers and lasers studied by simple analytical expressions," *Appl. Phys. Lett.* **52,** 1945-1947 (1988).

[4] Mao, M. -H. *et al.* "Study of high frequency response of self-organised stacked quantum dot lasers at room temperature," *Electron. Lett.* **33,** 1641–1642 (1997).

[5] Klotzkin, D. *et al.* "Enhanced modulation bandwidth (20 GHz) of $In_{0.4}Ga_{0.6}As$–GaAs self-organized quantum-dot lasers at cryogenic temperatures: role of carrier relaxation and differential gain," *IEEE Photon. Technol. Lett.* **10,** 932–934, (1998).

[6] Bhattacharya P. *et al.* "High-Speed modulation and switching characteristics of In(Ga)As–Al(Ga)As self-organized quantum-dot lasers," *IEEE J. Sel. Top. Quantum Electron*. **6,** 426–438 (2000).

[7] Liu, G. T. *et al.* "Extremely low room-temperature threshold current density diode lasers using lnAs dots in $In_{0.05}Ga_{0.85}As$ quantum well," *Electron. Lett.* **35**, 1163–1165 (1999).

[8] Shchekin, O. B. *et al.* "High temperature performance of a self-organized quantum dot laser with a stacked p-doped active region," *Electron. Lett.* **38**, 712–713 (2002).

[9] Asada M. *et al.* "Gain and the threshold of three-dimensional quantum-box lasers," *IEEE J. Quantum Electron.* **22,** 1915–1921 (1986).

[10] Newell, T. C. *et al.* "Gain and linewidth enhancement factor in InAs quantum-dot laser diodes," *IEEE Photon. Technol. Lett.* **11,** 1527–1529 (1999).

[11] Urayama, J. *et al.* "Observation of phonon bottleneck in quantum dot electronic relaxation," *Phys. Rev. Lett.* **86,** 4930–4933 (2001).

[12] Bayer, M. & Forchel A. "Temperature dependence of the exciton homogeneous linewidth in $In_{0.60}Ga_{0.40}As$/GaAs self-assembled quantum dots," *Phys. Rev. B.* **65,** 41308–41311 (2002).

[13] Matthews, D. R. *et al.* "Experimental investigation of the effect of wetting-layer states on the gain- current characteristic of quantum-dot lasers," *Appl. Phys. Lett.* **81,** 4904–4906 (2002).

[14] Krebs, R. *et al.* "High frequency characteristics of InAs/GalnAs quantum dot distributed feedback lasers emitting at 1.3μm," *Electron. Lett.* **37,** 1223–1225 (2001).

[15] Kamath, K. K. *et al.* "Small-signal modulation and differential gain of single-mode self-organized

$In_{0.4}Ga_{0.6}As$/GaAs quantum dot lasers," *Appl. Phys. Lett.* **70,** 2952–2953 (1997).
[16] Smowton, P. M. *et al. "*Filamentation and linewidth enhancement factor in InGaAs quantum dot lasers," *Appl. Phys. Lett.* **81,** 3251-3253 (2003).
[17] Uskov, A. V. *et al. "*Carrier-induced refractive index in quantum dot structures due to transitions from discrete quantum dot levels to continuum states," *Appl. Phys. Lett*, **84,** 272-274 (2004).
[18] Muszalski, J. *et al. "*Measurement of linewidth enhancement factor in self-assembled quantum dot semiconductor lasers emitting at 1310nm," *Electron. Lett.* **40,** 428-430 (2004).
[19] Markus, A. *et al. "*Impact of intraband relaxation on the performance of a quantum-dot laser," *IEEE J. Sel. Topics Quantum Electron*. **9,** 1308-1314 (2003).
[20] Mi, Z. & Bhattacharya, P. "DC and dynamic characteristics of P-doped and tunnel injection 1.65μm InAs quantum-dash lasers grown on InP (001)," *IEEE J. Quantum Electron.* **42,** 1224-1234 (2006).
[21] Martinez, A. *et al.* "Microwave frequency characterization of undoped and p-doped quantum dot lasers" *Appl. Phys. Lett.* **90,** 251101 (2007).
[22] Simpson, T. B. *et al.* "Small-signal analysis of modulation characteristics in a semiconductor laser subject to strong optical injection," *IEEE J. Quantum Electron.* **32,** 1465-1468 (1996).
[23] Lau, E. K. *et al.* "Frequency Response Enhancement of Optical Injection Locked Lasers," *IEEE J. Quantum Electron.* **44,** 90-99 (2008).
[24] Riou, B. *et. al.* IEEE European conference on optical communication, 2003
[25] Bossert, D. J. & Gallant, D. "Improved method for gain/index measurements of semiconductor lasers," *Electron. Lett.* **32,** 338–339 (1996)
[26] Harder, C. *et al.* "Measurement of the linewidth enhancement factor a of semiconductor lasers," *Appl. Phys. Lett.* **42,** 328-330 (1983).
[27] Naderi, N. A. *et al. "*Modeling the Injection-Locked Behavior of a Quantum Dash Semiconductor Laser," *IEEE J. Sel. Top. Quantum Electron*. **15,** 563-571 (2009).